

Excitation-induced dephasing and biexcitonic effects in the coherent control of excitonic polarization in pulse-transmission experiments

Tobias Voss,* Hans Georg Breunig, Ilja Rückmann, and Jürgen Gutowski

Institut für Festkörperphysik, Universität Bremen, P.O. Box 330 440, D-28334 Bremen, Germany

(Received 25 June 2003; revised manuscript received 26 November 2003; published 27 May 2004)

Optical coherent manipulation of excitonic polarization is studied in pulse-transmission experiments at medium to high excitation intensities. As a well-defined model system a ZnSe single-quantum well is used. It is found that for constant excitation intensities the dephasing time of the polarization in the sample changes significantly if the cases of coherent amplification and destruction are compared. This effect is explained in terms of an excitation-induced dephasing. The change of the dephasing time of the polarization is quantified. Furthermore, the simultaneous excitation of the exciton and exciton-biexciton resonances is shown to strongly influence the signal of the polarization in the coherent-control experiments. Both the excitation-induced dephasing and the biexcitonic effects are simulated by use of phenomenological models which give a good agreement with the experiments.

DOI: 10.1103/PhysRevB.69.205318

PACS number(s): 78.47.+p, 71.35.-y, 73.21.Fg

I. INTRODUCTION

Optical coherent control¹⁻⁴ has become a very promising tool in the last few years which could eventually provide ultra-high-speed all-optical switching devices.⁵ Such a technique is, for example, needed in the field of quantum-optical information processing where different quantum states must be addressed and manipulated with high precision on ultrashort time scales.^{6,7} One possibility to achieve this coherent control is to excite an appropriate system with two collinearly propagating phase-locked laser pulses, i.e., with two pulses whose relative phase can be tuned and stabilized with an accuracy of a fraction of their center wavelength.⁷⁻¹³ Depending on the relative phase the second pulse will either enhance or diminish the coherent optical polarization generated by the first pulse.

However, mainly two processes limit the time scale on which the coherent-control technique can be applied to a system: the lifetime of the quantum-mechanical excitation and the dephasing time of the optical polarization. For almost all cases the dephasing time is the main limiting factor since it is some orders of magnitude shorter than the lifetime. In semiconductor quantum wells, for example, the dephasing time of excitonic polarization, which is very well suited to study coherent-control mechanisms, is of the order of several picoseconds at a temperature of $T=4$ K (Refs. 8, 14, and 15) whereas the lifetime of the resulting exciton population can be within the nanosecond regime. Therefore, it is necessary to apply ultrashort laser pulses to achieve and study the coherent control in such samples.

It has been found in many previous experiments that the dephasing time of the induced optical polarization is not constant but noticeably depends on the excitation density.¹⁵⁻¹⁷ This so-called excitation-induced dephasing (EID) (Ref. 18) is known to strongly affect the optical response of semiconductor nanostructures and might be microscopically caused by different scattering processes such as exciton-continuum and two-pair-continuum scattering.¹⁰ This has been studied in different interferometric four- (Ref. 10) and six-wave-

mixing experiments¹⁹ on semiconductor quantum wells where the excitation-induced dephasing has been found to play an important role especially if the two pulses of the phase-locked pair overlap in time. It must be noted, however, that there is still a lack of an intuitively easy understanding of the underlying mechanisms. In previous work^{19,20} sophisticated microscopic models including phenomena of high order in the electric field have been used to explain the experimentally observed features. In another approach the semiconductor Bloch equations have been phenomenologically extended by an EID to reproduce these features.^{9,10} The main reason for the lack of an intuitive explanation is the complexity of transient four-wave-mixing experiments where an additional third pulse is applied to the sample to monitor the coherent control achieved with the phase-locked pulse pair in a background-free direction. Obviously, the interaction with this third pulse leads to a variety of further important microscopic processes which a theory must account for in order to be able to explain the experiment. Therefore, pulse-transmission experiments in which only the phase-locked pair of laser pulses is applied to a sample promise an easier interpretation of the underlying processes. Furthermore, a real-time resolved observation of the change of the dephasing time in coherent-control experiments should allow for a direct analysis of the effect of the EID in such experiments and has so far not been reported.

Another important fact which has to be taken into account is the existence of usually more than one single resonance in the sample. If ultrashort laser pulses (≤ 100 fs) which possess a spectral width of at least several meV are used for the coherent control, the simultaneous resonant excitation of two or more resonances lying in that energy range may lead to a complex interplay in the final optical response of the material. For the heavy-hole/light-hole exciton system this has already been studied in coherent-control experiments which make use of a pulse-transmission setup.⁸ The interplay of the simultaneous excitation of the exciton and exciton-biexciton resonance, however, has not been analyzed in pulse-transmission experiments with coherent control so far. In semiconductor quantum wells the transition from a one-

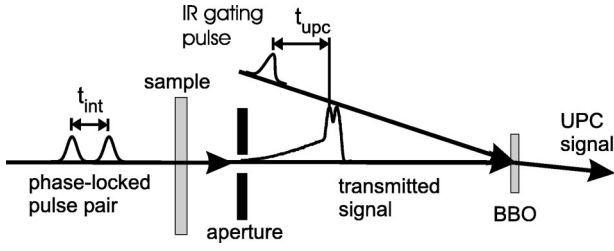


FIG. 1. Schematic experimental setup. The phase-locked pulse pair is generated by an actively stabilized Michelson interferometer (not shown). The real-time shape of the transmitted signal is measured by use of an up-conversion (UPC) technique. The UPC signal is either recorded for a fixed interpulse delay t_{int} as a function of t_{upc} which yields real-time transients of the transmitted signal or for a fixed t_{upc} as a function of Δt_{int} which yields the coherent-control signal.

exciton state to a bound biexciton state is usually excited together with the fundamental exciton transition.^{14,19,21,22} Therefore, it is important to analyze how the excitation of this additional resonance which is not independent of but strongly coupled to the fundamental exciton resonance will influence the coherent optical manipulation of the overall polarization in the sample.

In this paper we report on detailed experiments concerning the signal modifications resulting from the simultaneous excitation of the exciton and exciton-biexciton resonances and the influence of EID in coherent-control experiments. We apply the coherent control to a ZnSe single-quantum well which serves as an excellent model system to study the relevant mechanisms. However, the experimental results can be easily transferred to other systems to which coherent-control techniques are applied. The coherent control is studied in transmission geometry where the phase-locked pulses and the signal of the polarization are real-time resolved by use of a cross-correlation technique. With this experimental setup we directly show how the EID and the exciton-biexciton resonance influence the shape of the polarization transients. The EID shows its impact here even for fixed pulse intensities but different interpulse delays for which we are able to quantify the dephasing time. Furthermore, we analyze the intensity dependence of the observed features and compare them with simulations based on phenomenological models.

II. EXPERIMENTAL SETUP AND PROPAGATION OF A TRANSMITTED SINGLE PULSE

The experimental setup is shown in Fig. 1. The phase-locked pulse pair is generated by sending the pulses from a frequency-doubled, self-mode-locked Ti:sapphire laser through an actively stabilized Michelson interferometer. By this the temporal delay $t_{\text{int}} = t_{\text{int}}^0 + \Delta t_{\text{int}}$ between the two 120 fs (full width at half maximum) pulses can be tuned and stabilized with an accuracy of 40 as. t_{int}^0 denotes the basic interpulse delay time and Δt_{int} the fine tuning of the interpulse delay on a femtosecond time scale with a sub-femtosecond accuracy. A linear or circular polarization state of the pulse pair can be chosen by use of a Pockels cell. The pulse pair is then focused down to a spot size of $\approx 100 \mu\text{m}$

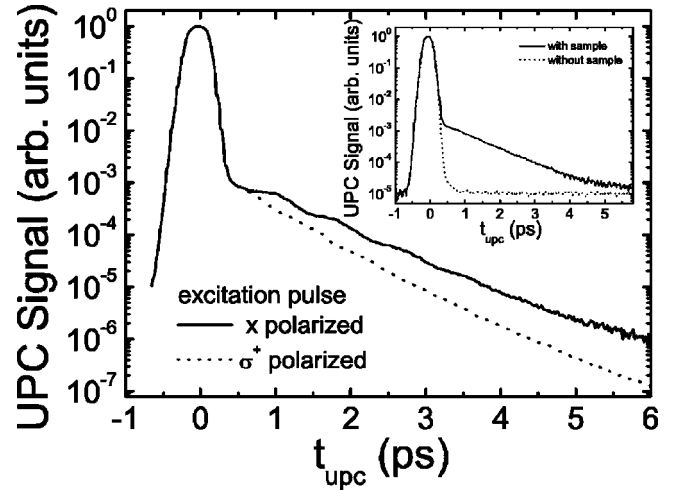


FIG. 2. Normalized up-conversion measurements of single pulses with an energy of 18 pJ. Exciton-biexciton beats are observed for linearly polarized excitation (solid line). For the excitation with a circularly polarized pulse (dot-dashed line) the formation of biexcitonic polarization is forbidden (beats are absent). The inset shows up-conversion measurements with and without the sample for a pulse energy of 1.2 pJ. All signals are shown on logarithmic scales.

and sent through the sample. The sample with a total thickness of about $1 \mu\text{m}$ consists of a ZnSe single-quantum well which is embedded into ZnSSe cladding layers. It was grown on an opaque GaAs substrate which thus had to be removed by wet chemical etching to allow for the experiments in transmission geometry. All experiments are performed at a temperature of $T = 4 \text{ K}$. The quantum well has a thickness of 10 nm and shows a sharp heavy-hole excitonic resonance at an energy of 2.826 eV which is $\approx 30 \text{ meV}$ below the lowest free-electron-hole transition. The relatively small spectral width of $\approx 15 \text{ meV}$ of the laser pulses allows for an exclusive excitation of this resonance together with its associated exciton-biexciton transition at 2.821 eV. The transmitted signal which consists of the laser pulses and a signal originating from the polarization which has been induced in the sample is then analyzed by use of a cross-correlation technique. The signal is overlapped noncollinearly with an additional IR gating pulse in a β -barium borate crystal. In the crystal the sum frequency of the signal and the gating pulse is generated (up-conversion technique, UPC). The gating pulse (central wavelength $\lambda_{\text{cent}} \approx 880 \text{ nm}$) is temporally scanned over the signal ($\lambda_{\text{cent}} \approx 440 \text{ nm}$) by changing the time delay t_{upc} . The sum-frequency signal ($\lambda_{\text{cent}} \approx 293 \text{ nm}$) is only generated in the temporal and spatial overlap region of the signal and the gating pulse. Due to phase matching conditions the sum-frequency signal is spatially separated from the signal and the gating pulse. The time resolution of the UPC technique is mainly given by the temporal width of the infrared gating pulse which was measured to be 100 fs.

Typical up-conversion measurements of the transmission of a single pulse (without the interferometer) through the ZnSe quantum well for a pulse energy of 18 pJ are shown in Fig. 2. Around $t_{\text{upc}} = 0 \text{ ps}$ the almost Gaussian shaped laser pulse can be observed (compare solid with dotted curve in

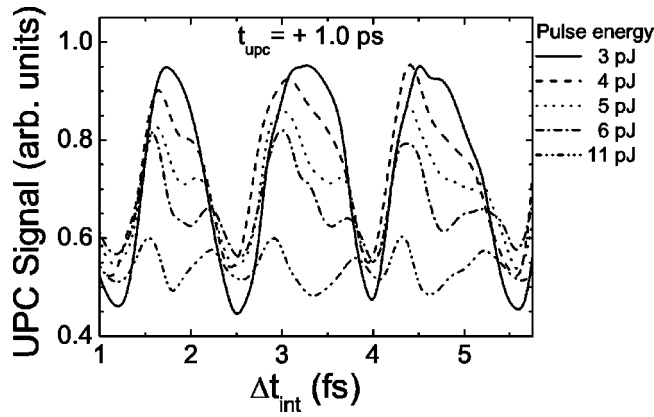


FIG. 3. Coherent-control signal as a function of Δt_{int} for $t_{\text{upc}} = +1.0$ ps and $t_{\text{int}}^0 \approx -300$ fs. As the pulse energy is increased, a reduction of the contrast ratio and additional minima at the position of the original maxima due to excitation-induced dephasing are observed.

the inset which were obtained with and without the sample for a low pulse energy of 1.2 pJ). After 400 fs the measured intensity has decreased by three orders of magnitude and the radiation of the polarization which has been induced in the sample by the pulse becomes visible. Due to dephasing processes the measured intensity now mainly decreases monoexponentially since predominantly the heavy-hole excitonic resonance was excited. The solid line corresponds to the transient measured for a linearly polarized excitation pulse, the dot-dashed line to that for a circularly (σ^+) polarized pulse. For the linearly polarized pulse the excitation of a bound-biexciton polarization is allowed in addition to the excitonic polarization. Therefore, exciton-biexciton beats are clearly visible and their origin can be verified in two ways. First, the beat period of 850 fs can be converted into an energy separation of $E_{xx} = 4.8$ meV between the two involved resonances. This separation exactly corresponds to the energy difference of the exciton and exciton-biexciton resonance observed in four-wave-mixing experiments. Second, the beats are not observed if a circular polarization state of the excitation pulse is chosen (dot-dashed line). In this case excitons are exclusively excited with one spin orientation which prevents the generation of a bound-biexciton polarization that requires opposite exciton spins.²³ The dephasing time T_2 is found to be slightly different for the two cases, i.e., 1.5 ps for the linear and 1.1 ps for the circular polarization state. The comparison of these T_2 times with $T_2 = 1.9$ ps obtained at low excitation intensity (1.2 pJ/pulse) shows that for high excitation intensity (18 pJ/pulse) EID significantly shortens the dephasing time of the excitonic polarization. The dephasing times have been calculated by assuming a predominantly homogeneous broadening of the resonances in the sample.

III. COHERENT CONTROL OF EXCITONIC POLARIZATION AND THE IMPACT OF EXCITATION-INDUCED DEPHASING

For the following coherent-control measurements a pulse pair obtained from the interferometer is used. The up-

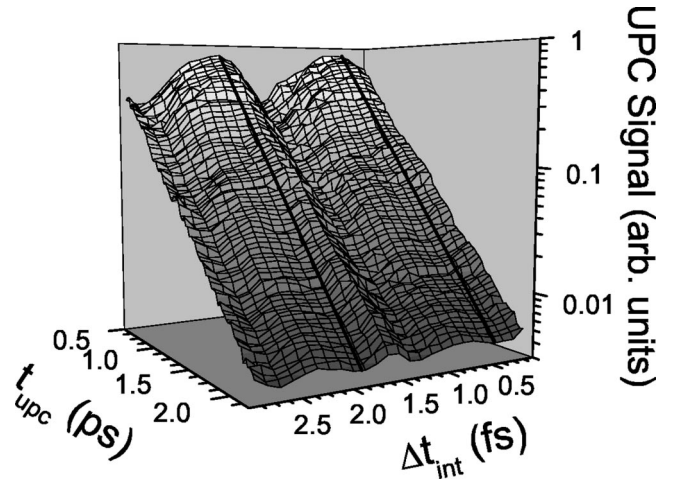


FIG. 4. Real-time transients (logarithmic signal scale) for different Δt_{int} demonstrating the occurrence of the fine structure due to excitation-induced dephasing. Cuts along the t_{upc} axis correspond to the real-time transients, cuts along the Δt_{int} axis yield coherent-control traces. Black lines: positions of constructive interference where for $t_{\text{upc}} > 1$ ps additional minima in the coherent-control traces occur. The pulse energy was 7 pJ.

conversion signal is either recorded for a fixed interpulse delay t_{int} as a function of t_{upc} to analyze the resulting transient of the phase-locked pulse pair in real time, or for a fixed t_{upc} as a function of Δt_{int} to analyze the coherent-control signal.

Figure 3 shows coherent-control signals for increasing pulse energies. For these measurements t_{upc} was fixed at +1.0 ps, t_{int}^0 was tuned to ≈ -300 fs, and the UPC signal was recorded as a function of the fine tuning of the delay Δt_{int} over a range of 5.7 fs. For an excitation energy of 3 pJ the coherent-control signal has still the shape of a cosinelike oscillation. This results from the successive change between constructive and destructive interference of the polarizations and occurs for linear interference conditions of the polarizations generated by the first and second pulse of the phase-locked pair, respectively. As the excitation energy is increased to 11 pJ per pulse the contrast ratio $(I_{\text{max}} - I_{\text{min}})/(I_{\text{max}} + I_{\text{min}})$ significantly decreases from 0.3 to 0.1. Simultaneously, additional minima evolve at those positions where for low excitation intensities maxima of the coherent-control signal occur. This fine structure observed in the coherent-control signal is similar to the one previously obtained in four- and six-wave-mixing experiments.^{9,19,20} For the theoretical explanation of the results of these wave-mixing experiments, the semiconductor Bloch equations were phenomenologically extended by an EID (Ref. 9) which results in an excellent agreement with the experiments. This implies that for constant excitation intensities a dependence of the dephasing time on the relative phase of the pulse pair should be directly observable which, however, has not been experimentally proven so far. The results presented in Fig. 2 furthermore strongly suggest that also in pulse-transmission experiments EID significantly modifies the coherent-control signal at medium to high excitation intensities and causes the additional fine structure.

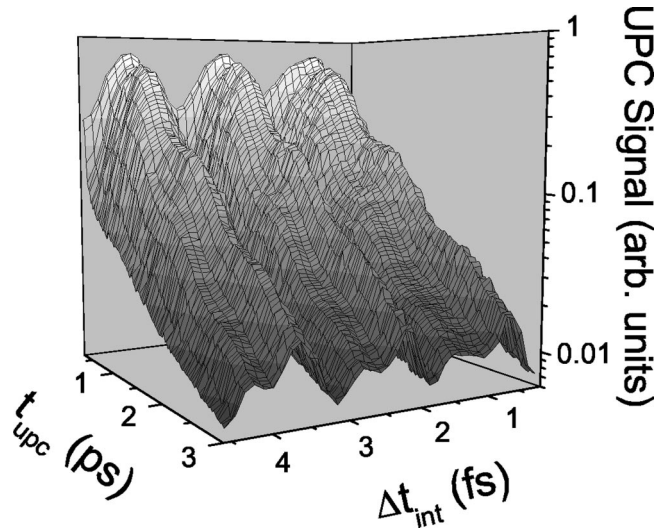


FIG. 5. Real-time transients (logarithmic signal scale) as a function of Δt_{int} for $t_{\text{int}}^0 \approx -430$ fs measured at a pulse energy of 25 pJ. Exciton-biexciton beats are clearly resolved on the transients. For $t_{\text{upc}} > 1.5$ ps the fine structure occurs in the coherent-control signal.

To directly show that the fine structure is indeed produced by EID, 28 real-time transients were recorded for different but fixed values of t_{int} around ≈ -300 fs for moderate excitation intensities ($E_{\text{pulse}} = 7$ pJ). After each measurement Δt_{int} was increased by ≈ 0.12 fs. In Fig. 4, the 28 transients are depicted on a logarithmic signal scale. In this plot the transients correspond to cuts along the t_{upc} axis, whereas the coherent-control signals can be extracted for fixed values of t_{upc} as cuts along the Δt_{int} axis. For $t_{\text{upc}} = 0.5, \dots, 1.0$ ps the coherent-control traces show the sinusoidal shape which is expected for linear interference of the polarizations induced by each pulse of the pulse pair. For $t_{\text{upc}} > 1.0$ ps, however, they exhibit additional minima at the positions of constructive interference (follow black lines in Fig. 4). These additional minima gradually evolve with increasing t_{upc} and are most distinctly visible in a range of $t_{\text{upc}} = 1.6, \dots, 2.2$ ps.

It becomes clear from Fig. 4 how the fine structure in the coherent-control signal is caused by EID. Although the constructive interference leads to maxima in the coherent-control signals for $t_{\text{upc}} < 1$ ps the faster decay due to dephasing of the large polarization just at these positions leads to the evolution of minima on the long-term scale, i.e., for $t_{\text{upc}} > 1$. This eventually yields a certain fine structure of the coherent-control traces. Obviously, also the contrast ratio in the coherent switching process is decreased by this effect. The most important fact, however, is that a significant effect of EID is directly observed here for a *constant* excitation intensity in a configuration where the phase-locked pulses are well separated in time which to our knowledge has not been reported so far. A phenomenological model that explains the observed effects in terms of exciton-exciton scattering at high densities will be discussed in Sec. VI.

IV. EXCITATION-INDUCED DEPHASING AND BIEXCITONIC EFFECTS

In order to increase the effect of the EID even more and quantify the change of the dephasing time T_2 as a function of

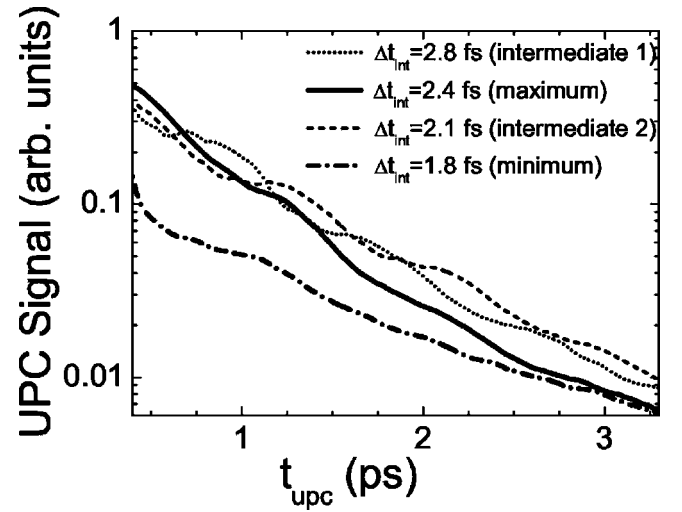


FIG. 6. Four transients from Fig. 5 (logarithmic signal scale) for constructive interference ($\Delta t_{\text{int}} = 2.4$ fs, solid line), two intermediate cases ($\Delta t_{\text{int}} = 2.1$ fs, dashed line and $\Delta t_{\text{int}} = 2.8$ fs, dotted line), and destructive interference ($\Delta t_{\text{int}} = 1.8$ fs, dot-dashed line).

Δt_{int} , the measurements shown in Fig. 4 were repeated under similar conditions, but for a higher pulse energy of $E_{\text{pulse}} \approx 25$ pJ. In this case the phase-locked pulses were separated by $t_{\text{int}}^0 \approx -430$ fs which corresponds to half the period of the exciton-biexciton beats in the sample (compare to Sec. II). The results obtained with these parameters are shown in Fig. 5. Now, the fine structure is even more distinctly visible than in Fig. 4. Additionally, exciton-biexciton beats are visible on the transients (cuts along the t_{upc} axis). Since the basic separation t_{int}^0 of the phase-locked pulses corresponds to $T_{\text{beat}}/2$ one would expect that, apart from the change of T_2 as a function of the fine tuning Δt_{int} , also a change of the amplitude and phase of the beat structure should occur in the coherent-control measurements.

To analyze these two effects Fig. 6 exemplarily shows four transients obtained from Fig. 5. The transient which corresponds to constructive interference of the induced polarizations (solid line) shows a much faster decay ($T_2 \approx 1.1$ ps) than the other three transients (dotted and dashed line $T_2 \approx 1.6$ ps, intermediate cases; dot-dashed line $T_2 \approx 1.8$ ps, destructive interference). This distinct difference in the dephasing times results in a crossing of the transients for constructive interference and for the intermediate cases at $0.7 \text{ ps} \leq t_{\text{upc}} \leq 1.0$ ps. This crossing leads to the fine structure in the coherent-control signals which thus can be observed for $t_{\text{upc}} > 1.0$ ps.

Furthermore, the transients which correspond to the intermediate cases (dashed and dotted line) show much stronger exciton-biexciton beats than the other two. At $t_{\text{int}}^0 \approx T_{\text{beat}}/2$ constructive interference for the exciton transition simultaneously implies destructive interference for the exciton-biexciton transition. Since the intensity of the excitonic polarization for linearly polarized excitation is usually several orders of magnitude larger than the biexcitonic polarization^{16,14} the overall strength of the measured signal in transmission experiments is dominated by the excitonic

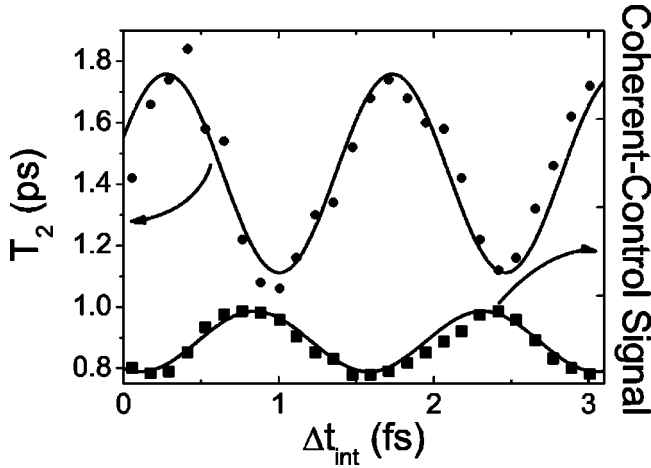


FIG. 7. Dephasing time T_2 of the polarization as a function of the interpulse fine-tuning delay time Δt_{int} (circles) extracted from the transients of Fig. 5 by numerical fitting. The squares show a corresponding coherent-control signal measured at a low excitation intensity for $t_{\text{upc}} = 1.0$ ps. The lines are best fits with cosine functions.

contribution. Consequently, a reduction of the exciton-biexciton beats should occur for the transients corresponding to constructive interference. Exactly this effect can be seen in Fig. 6. On the transient for destructive interference the beats are also weaker than in the intermediate case. This can be easily understood by considering that in this case much less excitonic polarization is excited than in the other two cases. This makes the formation of biexcitonic polarization by the absorption of an additional photon much more unlikely and consequently weakens the biexcitonic signatures in the signal. Additionally, the beat structures superimposed to transients corresponding to the intermediate cases show a relative phase shift of half a period. This phase shift is another clear indication of the separate control of the excitonic and biexcitonic polarizations. A phenomenological model that describes these effects in terms of two coupled oscillators will be discussed in Sec. VII.

V. QUANTITATIVE ANALYSIS OF THE EID

In order to analyze the effect of EID more quantitatively the dephasing time for each transient depicted in Fig. 5 has been extracted. The dephasing of the polarization together with the superimposed exciton-biexciton beats leads to a signal which can be phenomenologically described in the following way:

$$I(t) \propto \exp(-2t/T_2)[1 + C \sin(\omega t + \phi)] \quad (1)$$

The first factor describes the monoexponential decay of the measured signal $I(t)$ due to dephasing of the polarization with a decay time $T_2/2$ if a predominantly homogeneous broadening of the exciton resonance is assumed. The second factor describes the modulation of the decay with the exciton-biexciton beats where C gives the amplitude of the beats, ω ($\approx 7.4 \text{ ps}^{-1}$ in the present case) their frequency, and ϕ their phase.

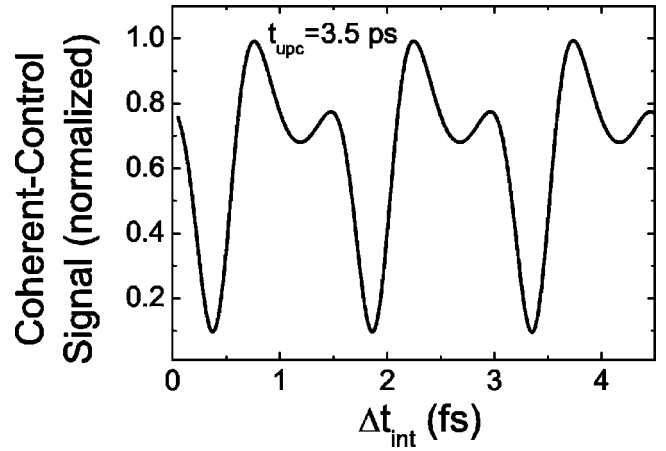


FIG. 8. Simulated coherent-control signal with a phenomenological EID accounting for exciton-exciton and exciton-continuum scattering as a function of Δt_{int} for $t_{\text{int}}^0 = -429.4$ fs. The model reproduces the experimentally observed fine structure. The parameter values are given in the text.

Figure 7 shows the dephasing time T_2 as a function of the interpulse fine-tuning delay Δt_{int} as extracted from Fig. 5 by numerically fitting each transient with Eq. (1) (circles) in comparison with a coherent-control measurement performed at a low excitation intensity for $t_{\text{upc}} = 1.0$ ps (squares). It is obvious that the dephasing time is strongly correlated with the coherent switching of the polarization because it oscillates with the same frequency. However, the two oscillations are clearly out of phase with a phase difference of $\approx \pi$. This means that for destructive interference the dephasing time has a maximum which in this experiment amounts to $T_2^{\text{max}} \approx 1.8$ ps. On the contrary, constructive interference of the induced polarization leads to a faster dephasing with $T_2^{\text{min}} \approx 1.0$ ps due to enhanced EID. Again it must be noticed that the change of the dephasing time of 44% is exclusively caused, for a *constant* excitation intensity, by the coherent-control process although the two phase-locked pulses are clearly separated in time by more than 400 fs. This evidently shows that the impact of EID on coherent-control experiments at medium to high excitation densities is not negligible and strongly alters the shape of the signal by adding a fine structure to the expected cosine oscillation. It also distinctively reduces the achievable contrast ratio in the coherent switching process.

In the following two sections phenomenological models will be discussed that describe the EID and the biexcitonic effects. Since the results in Fig. 4 show that the effect of EID occurs already at medium excitation intensities where biexcitonic effects are not yet observed, we will separately discuss the EID and the biexcitonic effects to simplify a direct comparison of the simulated and experimentally obtained features.

VI. MODEL: EID

To model the EID we use an approach similar to the one in Refs. 24 and 9. We neglect all propagation effects and describe the decay of the coherent excitonic polarization by

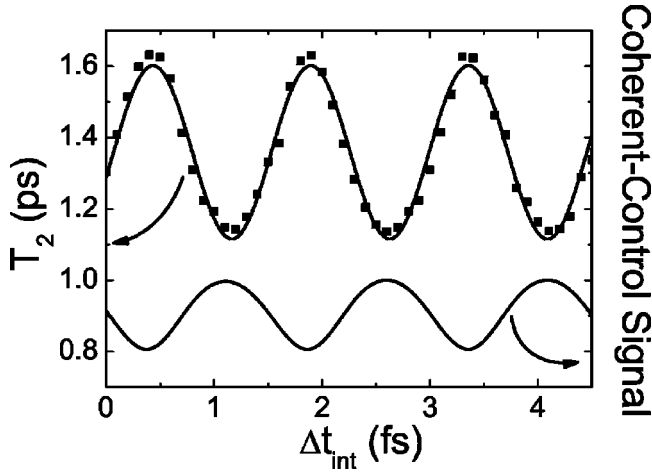


FIG. 9. Squares: calculated dephasing times T_2 as a function of Δt_{int} for $t_{\text{int}}^0 = -429.4$ fs. Upper solid line: numerical fit with a cosine function to the values of T_2 obtained with the simulation. Lower solid line: calculated coherent-control signal for low excitation intensities (i.e., change between constructive and destructive interference).

introducing a phenomenological dephasing rate γ . γ is expanded into Taylor series as a function of the excitonic f_{1s} and continuum population $\sum_n f_n$ where only the first nonconstant terms are kept:

$$\gamma = \gamma_0 + \gamma_1 f_{1s} + \gamma' \sum_n f_n. \quad (2)$$

The parameter $\gamma_0 = (1.9 \text{ ps})^{-1}$ is taken from the low-density experiments and γ_1 , γ' are taken as fitting parameters. Because of the relatively small spectral width of $\Delta E \approx 15$ meV of our laser pulses and the resonant excitation of the excitonic resonance we expect the exciton-exciton scattering to be the dominant process to lower the dephasing time of the polarization.

A simulated coherent-control signal is shown in Fig. 8. In the simulations the electric field was represented by two normalized Gaussian-shaped pulses with a temporal width of 120 fs and a separation of t_{int} . The result was obtained with $t_{\text{int}}^0 = -429.4$ fs, $t_{\text{upc}} = +3.5$ ps, $\gamma_1 = \gamma_0 / (6d^2)$ and $\gamma' = 10 \times \gamma_0 / d^2$ (d , dipole-matrix element). With this choice $d = \pi$ leads to a good agreement with the experimental results. The shape of the coherent-control signal is qualitatively in an excellent agreement with the experimental results shown in Fig. 3. The model of the EID is indeed able to reproduce the experimentally observed fine structure. Furthermore, the calculated signal shows a slightly asymmetric shape with respect to the “dip” at the position of constructive interference which is also observed in the experiments. By selectively switching off the exciton-exciton or the exciton-continuum scattering we were able to identify the exciton-exciton scattering to give a symmetric, but dominating contribution to the fine structure due to the lowering of the dephasing time precisely for constructive interference. The off-resonant contribution of the exciton-continuum scattering is found to only cause the slight asymmetry of the coherent-control signal as

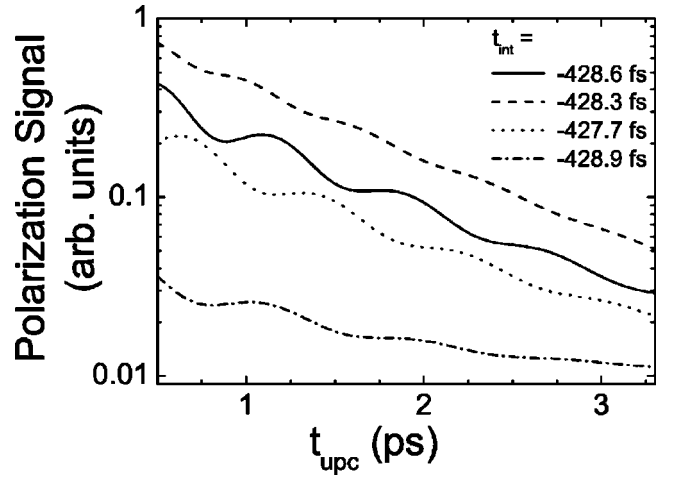


FIG. 10. Simulated polarization transients (logarithmic signal scale) around $t_{\text{int}} \approx -428$ fs for constructive interference (dashed line), two intermediate positions (solid and dotted lines), and destructive interference (dot-dashed line). The parameter values used for the simulation are given in the text.

it was expected from the argument based on the small spectral width of the laser pulses given above.

The phenomenological model is not only able to reproduce the shape of the coherent-control signal at medium to high excitation intensities. By extracting the dephasing time for each simulated transient we also obtain an excellent quantitative agreement of the simulated and experimentally found change of the dephasing time as a function of Δt_{int} . The result of the simulation with the parameter values given above is shown in Fig. 9. The simulation yields a continuous change of the dephasing time in the range of $1.10 \text{ ps} \leq T_2 \leq 1.65 \text{ ps}$ in good agreement with the experimentally observed range of $1.0 \text{ ps} \leq T_2 \leq 1.8 \text{ ps}$ shown in Fig. 7. The results of our simulations strongly support the interpretation of the experiments in terms of an excitation-induced dephasing of the excitonic polarization which is mainly caused by exciton-exciton scattering at medium to high excitation intensities. The additional influence of the exciton-biexciton transition of the shape of the transients at high excitation intensities will be modeled in the following section.

VII. MODEL: CONTROL OF BIEXCITON BEATS

In order to simulate the coherent manipulation of both the exciton and exciton-biexciton transitions we use an approach based on the average polarization model^{25,26} that has been previously applied to successfully simulate the coherent response of the exciton-biexciton system. The following two equations for the exciton transition amplitude Y and the bound-biexciton transition amplitude B are used to model the dynamics:

$$\begin{aligned} (\partial_t + \gamma_x + i\omega_x)Y &= idE + i\nu YYY^* + i\mu Y^*B, \\ (\partial_t + \gamma_{xx} + i\omega_{xx})B &= i\mu YY. \end{aligned} \quad (3)$$

These equations are obtained from a microscopic model based on the dynamics-controlled truncation scheme²⁷ by ne-

glecting the contributions from the exciton continuum as well as the Pauli blocking, and averaging over the k dependence. In the equations ω_x is the exciton frequency and $\omega_{xx} = 2\omega_x - E_{xx}/\hbar$ the frequency of the biexciton oscillator. For the following calculations their dephasing rates are assumed to be equal, $\gamma_x = \gamma_{xx} = (1.9 \text{ ps})^{-1}$. The polarization is driven by the electric field E in dipole coupling with the dipole-matrix element d . The term $i\nu YYY^*$ describes the Coulomb interaction and μ gives the strength of the nonlinear coupling of the two oscillators. For the following simulations $\nu = \mu^2 = 10^{-6}$ was chosen to achieve a good agreement with the experiment. The electric field and the dipole-matrix element were chosen according to the values given in Sec. VI.

Four simulated real-time transients of the polarization are shown in Fig. 10 for $t_{\text{int}} \approx -428 \text{ fs}$. To achieve a better agreement with the experiment a limiting background signal with a level of $10^{-2} \cdot I_{\text{max}}$ was added to the calculated signal where I_{max} denotes the signal intensity for $t_{\text{upc}} = 0.5 \text{ ps}$ at constructive interference.

The transients corresponding to intermediate positions (solid and dotted line) clearly show the strongest exciton-biexciton beats which is in excellent agreement with the experimental results presented in Fig. 6. At the positions of destructive (dot-dashed line) and constructive interference (dashed line) the beat amplitude is reduced. For the position of constructive interference this effect is due to the simultaneous destructive interference of the biexciton oscillator at the chosen value of $t_{\text{int}}^0 \approx -428 \text{ fs} \approx T_{\text{beat}}/2$. The reduction of the relative beat amplitude at the position of destructive interference is basically due to the finite background level. If this background is not added to the simulations also strong beats occur in this configuration which is, however, not observed in the experiment since they are superimposed on a signal which is a factor of ≈ 10 smaller than the background level in the experiment. The strong beats that occur in the simulation without a finite background level can be understood in the following way: at the position of destructive interference the contributions from the exciton oscillator are diminished and their overall strengths become more comparable to the strength of the biexciton oscillator thus leading to an increase of the beat amplitude. This is due to the fact that the destructive interference is always incomplete because of the dephasing of the polarization between the arrival of the first and second phase-locked pulse.

Furthermore, we also find an excellent agreement of the experiments and the simulations with respect to the phase shift of the exciton-biexciton beats that is observed for the two intermediate positions in Figs. 10 and 6. This phase shift again indicates that the exciton and exciton-biexciton resonances are separately coherently manipulated in the pulse-transmission experiments.

VIII. CONCLUSIONS

In conclusion, we have presented a detailed experimental and theoretical analysis of the impact of excitation-induced dephasing and the exciton-biexciton transition in all-optical coherent switching experiments. We have shown that for constant medium to high excitation intensities the change between constructive and destructive interference of the induced polarizations in the coherent switching process can very distinctly decrease the dephasing time of the polarization (in our case up to 44%). This result was obtained for a configuration where the two phase-locked pulses did not overlap in time, and it could be phenomenologically modeled by exciton-exciton scattering processes. By real-time resolving the time evolution of the excitonic polarization we were able to give an intuitive picture of how the EID gradually leads to a fine structure in the coherent-control signal as the time at which the signal is detected is increased. Furthermore, we found that the simultaneous excitation of the exciton-biexciton transition strongly affects the shape of the transients and the coherent-control signal. Exciton-biexciton beats on the transients were observed which could be enhanced or diminished in the coherent-control process. Again, a phenomenological model was able to reproduce the observed features. Our results show that excitation-induced dephasing and the influence of the exciton-biexciton resonance can be coherently manipulated in pulse-transmission experiments. Both effects strongly reduce the contrast ratio in the coherent all-optical switching process and modify the shapes of the transients.

ACKNOWLEDGMENTS

The authors thank W. Faschinger (deceased 2001), Würzburg University, for providing the sample. This work has been supported by the Deutsche Forschungsgemeinschaft (Grants Nos. Gu 252/12 and Ne 525/8) and the University of Bremen (BFK No. 1011).

*Email address: tvoss@ifp.uni-bremen.de

¹J.L. Herek, W. Wohlleben, R.J. Cogdell, D. Zeidler, and M. Motzkus, *Nature (London)* **417**, 533 (2002).

²R.N. Zare, *Science* **279**, 1875 (1998).

³A. Hache, Y. Kostoulas, R. Atanasov, J.L.P. Hughes, J.E. Sipe, and H.M. van Driel, *Phys. Rev. Lett.* **78**, 306 (1997).

⁴T. Froh Meyer and T. Baumert, *Appl. Phys. B: Lasers Opt.* **B71**, 259 (2000).

⁵A.P. Heberle, J.J. Baumberg, and K. Köhler, *Phys. Rev. Lett.* **75**, 2598 (1995).

⁶A. Ekert and R. Josza, *Rev. Mod. Phys.* **68**, 733 (1996).

⁷N.H. Bonadeo, J. Erland, D. Gammon, D. Park, D.S. Katzler, and

D.G. Steel, *Science* **1473**, 282 (1998).

⁸D.S. Yee, K.J. Yee, S.C. Hohng, D.S. Kim, T. Meier, and S.W. Koch, *Phys. Rev. Lett.* **84**, 3474 (2000).

⁹M.U. Wehner, J. Hetzler, and M. Wegener, *Phys. Rev. B* **55**, 4031 (1997).

¹⁰H.G. Breunig, T. Trüper, I. Rückmann, J. Gutowski, and F. Jahnke, *Physica B* **314**, 283 (2002).

¹¹A.V. Baranov, V. Davydov, A.V. Fedorov, M. Ikezawa, H.-W. Ren, S. Sugou, and Y. Masumoto, *Phys. Rev. B* **66**, 075326 (2002).

¹²P. Renucci, M. Paillard, X. Marie, T. Amand, J. Barrau, and C. Ciuti, *Phys. Status Solidi A* **178**, 373 (2000).

- ¹³N. Garro, M.J. Snelling, S.P. Kennedy, R.T. Phillips, and K.H. Ploog, *J. Phys.: Condens. Matter* **11**, 6061 (1999).
- ¹⁴B.M. Haase, U. Neukirch, J. Gutowski, G. Bartels, A. Stahl, J. Nürnberger, and W. Faschinger, *Phys. Status Solidi B* **206**, 363 (1998).
- ¹⁵B. Pal and A.S. Vengurlekar, *Phys. Rev. B* **66**, 155337 (2002).
- ¹⁶W. Langbein, T. Meier, S.W. Koch, and J.M. Hvam, *J. Opt. Soc. Am. B* **18**, 1318 (2001).
- ¹⁷J.A. Bolger, A.E. Paul, and A.L. Smirl, *Phys. Rev. B* **54**, 11 666 (1996).
- ¹⁸H. Wang, K. Ferrio, D.G. Steel, Y.Z. Hu, R. Binder, and S.W. Koch, *Phys. Rev. Lett.* **71**, 1261 (1993).
- ¹⁹T. Voss, H.G. Breunig, I. Rückmann, J. Gutowski, V.M. Axt, and T. Kuhn, *Phys. Rev. B* **66**, 155301 (2002).
- ²⁰H.G. Breunig, T. Voss, I. Rückmann, J. Gutowski, V.M. Axt, and T. Kuhn, *J. Opt. Soc. Am. B* **20**, 1769 (2003).
- ²¹W. Langbein and J.M. Hvam, *Phys. Rev. B* **61**, 1692 (2000).
- ²²H. Wang, J. Shah, T.C. Damen, and L.N. Pfeiffer, *Solid State Commun.* **91**, 869 (1994).
- ²³T.F. Albrecht, K. Bott, T. Meier, A. Schulze, M. Koch, S.T. Cundiff, J. Feldmann, W. Stolz, P. Thomas, S.W. Koch, and E.O. Göbel, *Phys. Rev. B* **54**, 4436 (1996).
- ²⁴M.U. Wehner, D. Steinbach, and M. Wegener, *Phys. Rev. B* **54**, R5211 (1996).
- ²⁵P. Kner, W. Schäfer, R. Lövenich, and D.S. Chemla, *Phys. Rev. Lett.* **81**, 5386 (1998).
- ²⁶U. Neukirch, S.R. Bolton, L.J. Sham, and D.S. Chemla, *Phys. Rev. B* **61**, R7835 (2000).
- ²⁷V.M. Axt and S. Mukamel, *Rev. Mod. Phys.* **70**, 145 (1998).